Gigahertz Modulation of Femtosecond Time-Resolved Surface Sum-Frequency Generation Due to Acoustic Strain Pulses

ARTICLE *in* THE JOURNAL OF PHYSICAL CHEMISTRY C · SEPTEMBER 2014

Impact Factor: 4.77 · DOI: 10.1021/jp503979c

4 AUTHORS, INCLUDING:

Lukasz Piatkowski
ICFO Institute of Photonic Sciences
26 PUBLICATIONS **264** CITATIONS
SEE PROFILE

Mischa Bonn
Max Planck Institute for Polymer Research
347 PUBLICATIONS **7,587** CITATIONS
SEE PROFILE

THE JOURNAL OF PHYSICAL CHEMISTRY C

Article

pubs.acs.org/JPCC

Gigahertz Modulation of Femtosecond Time-Resolved Surface Sum-Frequency Generation Due to Acoustic Strain Pulses

Cho-Shuen Hsieh,[†,‡] Huib J. Bakker,[†] Lukasz Piatkowski,[†] and Mischa Bonn*[,‡]

[†]FOM Institute AMOLF, Science Park 104, 1098 XG Amsterdam, The Netherlands

[‡]Max-Planck Institute for Polymer Research, Ackermannweg 10, 55128 Mainz, Germany

ABSTRACT: We study the properties of aqueous solution/air interfaces with time-resolved surface sum-frequency generation (SFG) spectroscopy. Using this technique, we monitor the change in SFG signal following the excitation of the water hydroxyl stretch vibrations with a strong ultrashort infrared pump pulse. We observe that, in addition to the excitation-induced changes in the signal resulting from vibrational excitation and relaxation on a time scale of picoseconds, the infrared excitation also induces a modulation of the SFG signal with a period of ∼180 ps. This modulation is caused by the interference between the SFG field directly radiated away from the air/liquid interface and the SFG field reflected or generated at the acoustic strain wavefront that is created by the infrared excitation pulse. The modulation is observed to be much stronger for aqueous salt solutions than for pure water, and the phase of the oscillations depends on the nature of the dissolved salt. This dependence of the phase can be explained from the differences in surface propensities of the ions of the different salts, giving rise to different net orientation of the interfacial water species.

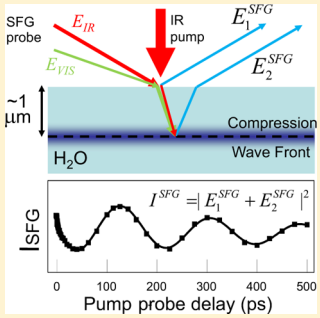

1. INTRODUCTION

Interfacial water molecules play a central role in heterogeneous catalytic processes in aqueous solutions and in interfacial biological processes like the aggregation of proteins at membrane−water interfaces. The termination of the hydrogen-bonded network of water at the interface makes the density and structure of interfacial water different from the bulk. The air/water interface, which is conceptually the simplest model of an aqueous interface, has been studied intensely in the past two decades.[1−8]

To explore the microscopic structure and dynamics of the water molecules at the air/water interface, vibrational sum-frequency generation (SFG) spectroscopy has been widely used. SFG is an even-order surface-specific optical technique, which provides the vibrational spectrum of the outermost few water monolayers.[1,9] In an SFG experiment, infrared (IR) and visible (VIS) pulses are overlapped at the interface both spatially and temporally. The SFG signal is enhanced when the IR light is resonant with one of the vibrational modes of the molecules at the interface. The non-hydrogen-bonded, free OH groups that are pointing into the air are characterized in the SFG spectrum of the air/water by a relatively sharp peak at 3700 cm^{-1}.[5,10] This spectral feature is unique to the interface of water and hydrophobic materials. The SFG spectrum of air/water interfaces further shows a broad 3100−3600 cm^{-1} band due to hydrogen-bonded (H-bonded) OH groups. In recent years, it has become possible to perform SFG spectroscopic studies with femtosecond laser pulses, which also enables the use of time-resolved SFG (tr-SFG) to study the structural and vibrational dynamics of water molecules at interfaces.

In a time-resolved SFG (tr-SFG) intense ultrashort infrared pulses are employed to excite a specific molecular vibration of a significant fraction (typically ∼10%) of the molecules at the interface. The effect of this excitation is measured with a time-delayed SFG probe pair. Since the SFG signal originates specifically from the surface molecules, tr-SFG enables the selective study of the dynamics of the outermost molecular layer.[2−4,11−17]

The tr-SFG technique, including polarization-resolved[3] and two-dimensional tr-SFG, has been applied to several systems in the past few years.[13,15,18,19] In all tr-SFG experiments the excitation by the infrared pump pulse leads to an ultrafast change in intensity and spectral dependence of the SFG signal. The subsequent evolution in amplitude, spectral dependence, and anisotropy of the SFG signal change provides unique information on the vibrational relaxation, spectral diffusion, molecular reorientation, and thermalization of the molecules at the surface. For aqueous interfaces these dynamics typically occur on subpicosecond to picosecond time scales.[3,4,18]

While the SFG probe is surface-specific, the IR excitation pulse is not and will excite (in the O−H stretch region) the vibrations of water molecules down to typically ∼1 μm into the bulk. This bulk excitation is converted into heat on the time scale of vibrational relaxation, i.e., a few picoseconds.[20,21] Thermal diffusion of heat away from the excitation region occurs on much longer time scales. Hence, the excitation with an ultrashort femtosecond infrared laser pulse leads to locally hot water at a temperature that remains constant within the typical nanosecond time window of time-resolved experiments.

Received: April 23, 2014
Revised: July 16, 2014
Published: August 18, 2014

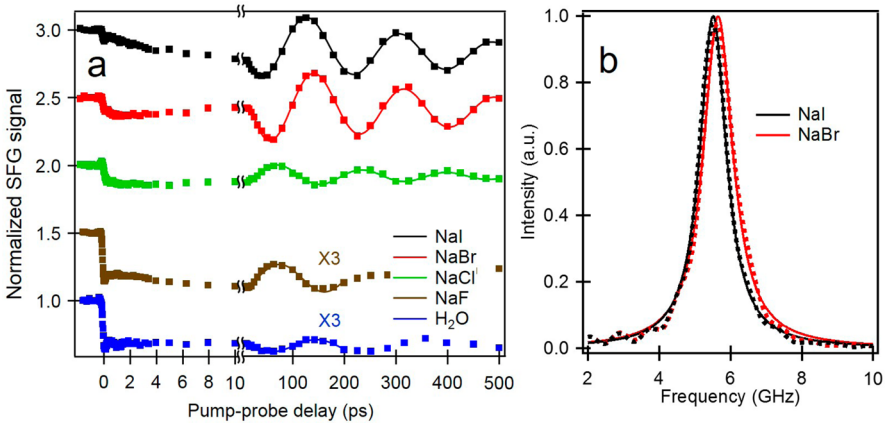

Figure 1. (a) IR-pump/SFG-probe data for hydrogen-bonded OH at air/water interface for pure H_2O and various sodium halide solutions, in the order of increasing size of the halide anions. The solid lines are fits to the data after 10 ps using exponentially damped sine functions. The data are offset vertically by multiples of 0.5 (0.5 for NaF, 1 for NaCl, 1.5 for NaBr, and 2 for NaI) and multiplied by indicated factors (factors of 3 for both H_2O and NaF) for clarity. The −1.8 to 10 ps parts are enlarged to show the transient decrease due to the excitation of the population from the ground to the first excited vibrational state. (b) Normalized Fourier transforms of the time-resolved data of the NaI and NaCl (dotted trace) and fits of the spectra to Lorentzians (solid lines).

In time-resolved studies of aqueous systems the heating effect reveals itself as a blue-shifted spectrum at long delay times.[17]

In a recent tr-SFG study of aqueous salt solutions, the vibrational energy relaxation of the water vibrations was observed to be followed by strong signal oscillations with a long period of ∼180 ps.[19] Here we investigate the nature of these oscillations by varying the composition of the aqueous solution, the nature of the solvent, and the geometrical parameters of the experiment. We find strong evidence that the slow oscillations of the tr-SFG signal are due to the generation of an acoustic strain pulse that is launched into the bulk water from the interface immediately upon vibrational relaxation and energy dissipation.

2. MATERIALS AND METHODS

The laser system consists of a Ti:sapphire oscillator (Mira, Coherent) seeding a regenerative Ti:sapphire amplifier (Titan, Quantronix). The amplifier is pumped by a high-energy Nd:YLF laser (Evolution, Coherent). The output of the amplifier was centered at 806 nm with a full width at half maximum (FWHM) of 12 nm and a pulse duration of 100 fs. The multipass amplifier produces ∼3 mJ of energy per pulse with a repetition rate of 1 kHz. A commercial optical parametric amplifier (TOPAS, Light Conversion) was pumped with 1 mJ of the amplified 806 nm beam to produce signal and idler fields, with idler wavelengths at 2208 and 2019 nm, from which IR frequencies of 3350 and 2500 cm^{-1} are generated (see below) to perform experiments on H_2O and D_2O samples, respectively. The idler was frequency-doubled in a β-barium borate (BBO) crystal. The doubled idler was mixed with 2 mJ of the 806 nm Ti:sapphire output in a difference frequency generation process in a $KTiOPO_4$ (KTP) crystal to produce mid-IR pulses centered at 3350 and 2500 cm^{-1}. The generated IR beam was split 80/20 for IR pump and SFG probe purposes. The visible probe beam was formed from small portion of the amplifier output (0.1 mJ, 806 nm). The IR-pump/SFG-probe measurements were performed in reflection geometry. The VIS probe, IR probe, and IR pump beams lay in the same plane, orthogonal to the air/sodium halide solutions interface, with incident angles of 50°, 45°, and 55° relative to the surface normal, unless otherwise specified, and are focused down to a beam waist of 100, 100, and 150 μm, respectively. The energies of the IR pump, IR probe, and VIS probe at the sample were 32, 8, and 4 μJ/pulse, respectively.

The samples were NaI, NaBr, NaCl, and NaF dissolved in distilled Millipore filtered water (18MΩ·cm resistivity) or D_2O (Cambridge Isotope Laboratories, Inc., 99.93% purity, used without further purification) with a mole fraction of $0.036x$ (∼2.1 M) for NaI, NaBr, and a lower mole fraction of NaCl solutions and $0.015x$ (∼0.85 M) for the NaF solution because of the limited solubility of NaF in water. The samples were placed in a homemade Teflon trough which was rotated at 8 rpm to refresh the sample between shots, to reduce the effect of cumulative heating. The IR-pump/SFG-probe spectra were recorded under p/ssp (IR pump/SFG, VIS probe, IR probe) polarization. The IR pump pulse was variably delayed with respect to the SFG probe signal passing the pulse over a mechanical delay line. The normalized IR-pump/SFG-probe signal was computed as the ratio between the integrated intensities with and without the pump.

3. RESULTS

In Figure 1a we show results from IR-pump/SFG-probe experiments for pure H_2O and NaF, NaCl, NaBr, and NaI solutions, in the order of increasing size of the halide anions. At short times after the excitation (within 2 ps), the normalized SFG signals show a transient decrease due to the excitation of population from the ground to the first excited vibrational state. After 10 ps, the data show slow, long-living oscillations that are damped on a time scale of several nanoseconds. The solid lines are fits to the data after 10 ps to a damped sine function, i.e., to $I(t) = -Ae^{-(t/T)} \sin(t/\tau + \Delta\varphi) + B$, where A is the amplitude of the oscillation, T is an exponential damping time constant, τ is the oscillation period, $\Delta\varphi$ is the initial phase, and B is an amplitude offset. The parameters resulting from the fits are listed in Table 1. The oscillation periods τ are nearly the same (∼175 ps) for all samples, evidently not particularly sensitive to the halide ion species, while the phase $\Delta\varphi$ does depend on the nature of the dissolved salt.

The amplitude of the oscillation increases as the size of the anion increases. This is attributed to the fact that aqueous solutions of NaCl, NaBr, and NaI exhibit, in that order, an

dx.doi.org/10.1021/jp503979c | J. Phys. Chem. C 2014, 118, 20875−20880

Table 1. Period of Oscillation (τ) and the Phase Shift ($\Delta\varphi$) of IR-Pump/SFG-Probe Data for Different Sodium Halide Solutes in H_2O[a]

solution	period of oscillation τ (ps)	phase shift $\Delta\varphi$ (rad)
0.036x NaI	179 ± 1	0.18 ± 0.02
0.036x NaBr	174 ± 1	−0.45 ± 0.03
0.036x NaCl	164 ± 2	1.96 ± 0.05
0.015x NaF	174 ± 4	2.05 ± 0.09
pure H_2O	182 ± 3	−0.36 ± 0.06

[a]The phase shift is defined relative to the negative sine wave.

increasingly strong enrichment of halide anions at the interface compared to the bulk, thus causing a significant amount of charge to be present at the surface with a corresponding distortion of the H-bonding network and an enhancement of the SFG signals. The interfacial water structures for NaF and, to a lesser extent NaCl, aqueous solutions are roughly the same as the interfacial structure of the air/water interface.[22] Figure 1b shows the Fourier transform of the tr-SFG data of the NaI and NaBr solutions. The Lorentzian spectral shape with a central frequency of ~5.7 GHz corresponds to the exponentially damped sinusoidal waves with a period of ~175 ps observed in Figure 1a. The width of the Lorentzian spectral lines correspond to damping time constants of 352 and 316 ps for the NaI and NaBr solutions, respectively.

Figure 2a shows the oscillations of the SFG signal for different IR pump energies in the 0.036x NaI solution. In Figure 2b we show the amplitude of the oscillation as a function of the IR pump energy. As the IR pump energy is reduced from 21 through 14 to 7 μJ per pulse, the amplitudes of the oscillations decrease proportionally, while the period remains unchanged. In Figure 3 we present the results of measurement

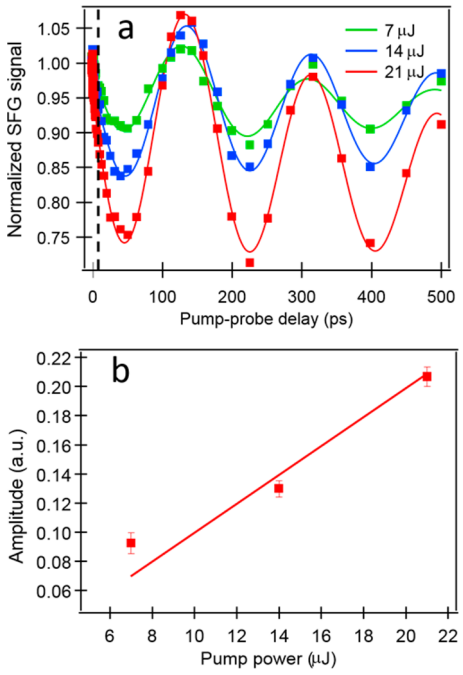

Figure 2. (a) Tr-SFG data for the 0.036x NaI solution, for pump powers of 7, 14, and 21 μJ. The solid lines are fits of the data to damped sine functions. The dashed black line indicates the 10 ps time point where the fitting starts. (b) Amplitudes of the oscillations as a function of IR pump energy.

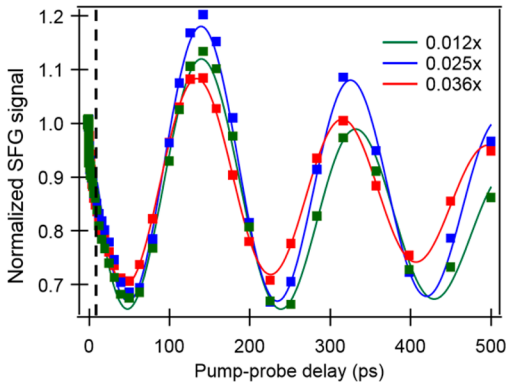

Figure 3. Tr-SFG data for different concentrations of NaI. The amplitude and the oscillation period are very similar for 0.012x, 0.024x, and 0.036x NaI solutions.

for different concentrations of NaI, ranging from 0.012x to 0.025x to 0.036x. Interestingly, the signal shows very little change either in amplitude, in phase, or in the oscillation period. This finding suggests that the surface concentration of iodide hardly changes when the bulk concentration is varied within this high concentration range, which implies that the surface would be saturated with halide ions.

Figure 4 shows the IR-pump/SFG-probe traces of a 0.036x NaI solution measured with two different incident angles for

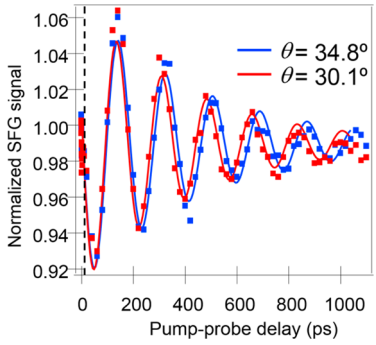

Figure 4. Tr-SFG data measured with different incident angles of the IR/VIS SFG probe pair. The period of the oscillation is proportional to sec θ, where θ is the refracted angle of the SFG signal. The solid lines are the fitted curves.

the SFG probe pulse pair. The red data are obtained with incident angles of the IR probe = 37.0° and VIS probe = 42.9°, which leads to a reflected angle of 41.7° and a refracted angle of 30.1° of the SFG signal. The blue data are obtained with incident angles of the IR probe = 44.6° and VIS probe = 50.4°, which leads to a reflected angle of 49.2° and a refracted angle of 34.8° of the SFG signal. The oscillation period clearly depends on the incident angles: for the red data the period is 175 ± 1 ps, while for the blue data the period is 183 ± 1 ps.

Figure 5 shows the IR-pump/SFG-probe traces of a 0.036x NaI solution in H_2O (red curve) and in D_2O (blue curve). The oscillation periods are 177 ± 1 ps for H_2O (red curve) and 193 ± 2 ps for D_2O (blue curve) and thus clearly depend on the nature of the solvent.

4. DISCUSSION

The oscillations can be well explained from an interference effect of SFG light that is directly generated at the surface and

dx.doi.org/10.1021/jp503979c | J. Phys. Chem. C 2014, 118, 20875−20880

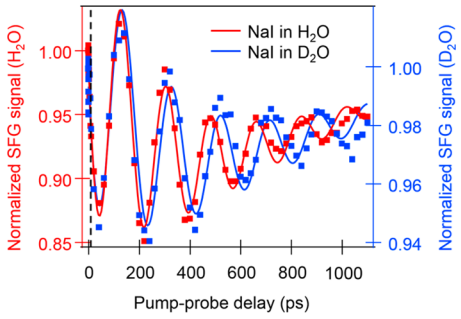

Figure 5. Tr-SFG data for NaI in H_2O and D_2O solvents. The solid lines are fits of the data to damped sine functions.

SFG light that is reflected from, or generated at, the density fluctuations associated with an acoustic strain pulse. Acoustic strain pulses are fast mechanical transients generated by sudden compression of the material, causing a weak leading edge followed by a stronger, faster trailing edge, which constitutes the wavefront.[23] The investigation of acoustic strain waves provides information on the hydrodynamic properties of the bulk medium such as the flow of pressure, temperature, and density. Femtosecond pulses can initiate an acoustic strain pulse at a well-defined moment and enable the detailed study of the mechanism of acoustic wave generation.[23,24]

As shown in Figure 6, the IR pump pulse hits the surface, resonantly excites the O−H stretch vibrations, and is absorbed

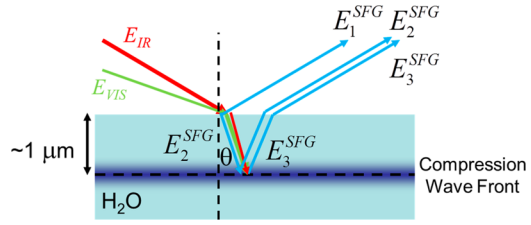

Figure 6. Schematic diagram of the experiment. The IR pump pulse produces a compression wavefront propagating into the bulk. The oscillations originate from the interference between the SFG field generated at the solution/air interface E_1^{SFG} and the propagating SFG field E_2^{SFG} that is reflected from the compression wavefront and/or the SFG field E_3^{SFG} that is generated at the compression wavefront .

in the first ~micrometer of the solution. Following vibrational relaxation, this layer of the solution is heated (by ~10 °C) on a time scale of ~1 ps. The thermal expansion associated with this quasi-instantaneous heating creates an acoustic strain pulse. The compression wavefront propagates into the bulk solution and travels with acoustic velocity v.

There are two different mechanisms by which the compression wavefront forms an additional source of SFG light that interferes with the SFG light directly generated at the surface. In the first mechanism, part of the SFG field generated at the surface (E_1^{SFG}) is transmitted into the bulk phase and partially reflected (E_2^{SFG}) from the compression pulse wavefront due to the density difference between the wavefront and the surrounding environment. The oscillations in the SFG signal intensity would—in this scenario—be attributed to the interference of two SFG fields E_1^{SFG} and E_2^{SFG}. As time progresses, the path length, and thereby the phase, of the E_2^{SFG} field increases, resulting in time-dependent constructive and destructive interference between E_1^{SFG} and E_2^{SFG}, giving rise to temporal oscillations of the signal. In this scenario, the damping of the signal would be caused by spatial broadening of the wavefront, reducing the reflectivity of the SFG field from the wavefront, and reducing the E_2^{SFG} field intensity. In the second scenario, the transmitted VIS/IR probe pulses generate another SFG field E_3^{SFG} at the compression pulse wavefront. This generation is enabled by the density difference between the wavefront and the surrounding water, leading to an asymmetric dielectric environment. In this scenario, the oscillations in the SFG signal intensity are attributed to the interference of the two SFG fields E_1^{SFG} and E_3^{SFG}.

The amplitude of the oscillations increases linearly with the energy of the IR pump pulse (Figure 2), which indicates that the density modulation associated with the acoustic strain pulse is proportional to the incident IR pump power. The refractive indices of water at frequency ω, $n(\omega)$, equal 1.33, 1.33, and 1.34 respectively for the SFG, VIS, and IR pulses used in our experiment.[25] This means that dispersion effects are negligible, and the optical path difference between the E_1^{SFG} on one hand and E_2^{SFG} and E_3^{SFG} on the other is $2Ln(\omega)\cos\theta$, where L is the distance between the air/water interface and the acoustic pulse wavefront and θ is the angle of refraction of the SFG signal (see Figure 6). The distance between the air/water interface and the acoustic pulse wavefront increases in time as $L = vt$, where v is the acoustic velocity of the solution and t is the time interval after the acoustic strain pulse is launched. The observed oscillation period corresponds to the time interval in which the optical path difference of the sources E_1^{SFG} and E_2^{SFG}/E_3^{SFG} equals the wavelength of the probe SFG signal, so $\tau = \lambda/2vn\cos\theta$, where τ is the period of the oscillation signal and λ is the wavelength of the SFG signal.

This expression for τ accounts very well for the observed oscillation periods. The frequency of the IR probe is 3350 cm^{-1} and the wavelength of the VIS probe is 806 nm, which leads to an SFG signal with a wavelength of 634.6 nm. The incident angles of IR probe = 44.6° and VIS probe = 50.4° correspond to a refracted angle θ of 34.7° of the SFG signal. The acoustic velocity of H_2O is 1496 m/s. With these parameters we calculate the oscillation period of H_2O to be ~190 ps, in quite good agreement with the experimentally observed oscillation times (Table 1).

The expression for τ also accounts very well for the observed dependence of the oscillation period on the incident angles. In Figure 4 we showed that the oscillation period changes from 175 ± 1 to 183 ± 1 ps when the refracted (internal) angle θ changes from 30.1° to 34.8°. The ratio of the oscillation periods (0.956) is indeed very close to the ratio of the values of $1/\cos\theta$ (0.949). The expression for τ also explains the dependence of the oscillation period on the nature of the solvent (Figure 5). For a solution of NaI in D_2O solution, the IR pump and probe are both centered at 2500 cm^{-1}, leading to an SFG signal at 670.5 nm. The acoustic velocity of D_2O is 1400 m/s. Hence, the ratio of λ_{SFG}/v changes by a factor 1.1 going from H_2O to D_2O, which agrees with the observed increase of the oscillation period by ~10% from 177 ± 1 ps for H_2O to 193 ± 2 ps for D_2O.

While we cannot definitively distinguish between E_2^{SFG} and E_3^{SFG} as the source of the field interfering with E_1^{SFG}, the observed damping of the oscillations indicates that E_3^{SFG} is the more likely source, i.e., $E_3^{SFG} \gg E_2^{SFG}$. The damping time of 352 ps deduced from Figure 1b corresponds to an optical penetration depth of 0.53 μm, which corresponds well to the exponential optical penetration depth of the IR pulse at 3350 cm^{-1} in water (0.6 μm)[26] (the difference may be explained by

dx.doi.org/10.1021/jp503979c | J. Phys. Chem. C 2014, 118, 20875−20880

an additional contribution to the damping by the broadening of the wavefront of the acoustic strain pulse). The broadening of the wavefront (which would be responsible for damping in case $E_2^{SFG} \gg E_3^{SFG}$) is expected to occur on longer (~nanoseconds) time scales, as has been shown with linear reflectivity experiments.[27]

If E_2^{SFG} were the interfering SFG field, the modulation would originate from the reflection of the SFG beam. In Figure 1, the amplitude of the oscillation for NaI trace, for example, is 0.3, which means that E_2^{SFG} in Figure 6 amounts to $\sim 0.16E_1$. Since the reflection and transmission signals generated at the interface are roughly equal,[28] the reflectivity at the wavefront would have to be ~0.16. Such a reflectivity would require a refractive index of 1.68 at the water wavefront, which is unphysically large.

A third indication that E_3^{SFG} constitutes the interfering SFG field is the observation that the phase shift $\Delta\varphi$ differs for the different solutions, as shown in Table 1. The NaBr and NaI solutions and pure water have an initial phase $\Delta\varphi$ around 0 rad, while NaCl and NaF show initial phases $\Delta\varphi$ around 2 rads. The phase shift represents the phase difference between the two SFG fields. If the oscillations were caused by interference of fields E_1^{SFG} and E_2^{SFG}, the relative phase is not expected to change between different solutions as E_2^{SFG} is the reflection of E_1^{SFG}. Such a solution-dependent phase difference is possible in case the interfering field is formed by the generated SFG field E_3^{SFG} because the phase (sign) of the second-order susceptibility $\chi^{(2)}$ at the surface can differ from the phase of $\chi^{(2)}$ at the compression wavefront of the acoustic strain pulse. The surface activities of the different halide ions and their effect on the orientation of interfacial water molecules are known to depend on the size and polarizability of the halide ion. The modulation of the microscopic structure of the water interface by ions has been addressed previously; theoretically, MD simulations have shown that larger anions with larger polarizabilities are enriched at the air/water interface.[29,30] Experimentally, SFG spectra show that large anions cause significant distortion of the surface hydrogen-bonding network.[19,22] As a result, the imaginary part of the surface susceptibility changes sign when larger halides are present in solution (specifically iodide[31]). This sign change is likely the result of the high surface propensity of the larger halide anions and would thus not be present for the SFG signal generated at the compression wavefront, at which the halide anion concentration has the bulk value. Hence, the difference in halide ion concentration at the surface and in the bulk may explain the π phase shift between E_1^{SFG} and E_3^{SFG} between the smaller and larger halide ions. Within this scenario, we cannot, however, rationalize the similarity in phase observed at the pure water interface and the large halide ions.

Irrespective of the precise origin of the interference effect, it is apparent that the occurrence of the signal oscillations must be accounted for in the interpretation of ultrafast time-resolved, ultrafast sum-frequency generation experiments, as described in more detail in the Supporting Information of ref 19.

5. CONCLUSIONS

We observe long-living oscillations of the signal measured in tr-SFG (IR-pump/SFG-probe) spectroscopic experiments of the interface of air and aqueous solutions. We study the origin of these oscillations by varying the composition of the solution and the experimental geometry. We find strong evidence that the oscillations are due to an interference effect of the SFG signal generated at the surface and SFG light that is reflected or generated at the propagating density profile of an acoustic strain pulse. This acoustic strain pulse is launched into the bulk water from the interface immediately upon vibrational relaxation and energy dissipation. The period of the oscillations is inversely proportional to the sound velocity and is similar for pure H_2O and solutions of NaF, NaCl, NaBr, and NaI in H_2O. The amplitude of the oscillations increases with increasing size and polarizability of the halide ion. The initial phase of the oscillations depends on the nature of the halide ion. This dependence may be explained from the fact that the phase of the second-order susceptibility $\chi^{(2)}$ and thus the phase of the generated SFG field depends on the local concentration of halide ions. Larger halide ions like Br^- and I^- have a high surface propensity, and thus for solutions of these ions there can be a large phase difference between the SFG field generated at the surface (that depends on the surface concentration of the halide ions) and the SFG field generated at the compression wavefront of the acoustic strain pulse (that depends on the bulk concentration of the halide ions).

AUTHOR INFORMATION

Corresponding Author

*E-mail bonn@mpip-mainz.mpg.de (M.B.).

Present Addresses

C.-S.H.: Physical Chemistry Department - Sciences II - University of Geneva, 30, Quai Ernest Ansermet, CH-1211, Geneva 4, Switzerland.

L.P.: ICFO—Institut de Ciencies Fotoniques, Mediterranean Technology Park, 08860 Castelldefels, Barcelona, Spain.

Notes

The authors declare no competing financial interest.

ACKNOWLEDGMENTS

We are grateful to Dr. D. Dlott, Dr. Y.-R. Shen, and Dr. Y. Nagata for fruitful discussions throughout the course of this study.

REFERENCES

(1) Du, Q.; Superfine, R.; Freysz, E.; Shen, Y. R. Vibrational Spectroscopy of Water at the Vapor/Water Interface. *Phys. Rev. Lett.* **1993**, *70*, 2313−2316.

(2) McGuire, J. A.; Shen, Y. R. Ultrafast Vibrational Dynamics at Water Interfaces. *Science* **2006**, *313*, 1945−1948.

(3) Hsieh, C.-S.; Campen, R. K.; Vila Verde, A. C.; Bolhuis, P.; Nienhuys, H.-K.; Bonn, M. Ultrafast Reorientation of Dangling OH Groups at the Air-Water Interface Using Femtosecond Vibrational Spectroscopy. *Phys. Rev. Lett.* **2011**, *107*, 116102.

(4) Hsieh, C.-S.; Campen, R. K.; Okuno, M.; Backus, E. H. G.; Nagata, Y.; Bonn, M. Mechanism of Vibrational Energy Dissipation of Free OH Groups at the Air-Water Interface. *Proc. Natl. Acad. Sci. U. S. A.* **2013**, *110*, 18780−18785.

(5) Raymond, E.; Tarbuck, T.; Richmond, G. Isotopic Dilution Studies of the Vapor/Water Interface as Investigated by Vibrational Sum-Frequency Spectroscopy. *J. Phys. Chem. B* **2002**, *106*, 2817−2820.

(6) Watanabe, H.; Yamaguchi, S.; Sen, S.; Morita, A.; Tahara, T. "Half-Hydration" at the Air/Water Interface Revealed by Heterodyne-Detected Electronic Sum Frequency Generation Spectroscopy, Polarization Second Harmonic Generation, and Molecular Dynamics Simulation. *J. Chem. Phys.* **2010**, *132*, 144701.

(7) Tian, C.-S.; Shen, Y. R. Isotopic Dilution Study of the Water/Vapor Interface by Phase-Sensitive Sum-Frequency Vibrational Spectroscopy. *J. Am. Chem. Soc.* **2009**, *131*, 2790−2791.

(8) Nagata, Y.; Hsieh, C.-S.; Hasegawa, T.; Voll, J.; Backus, E. H. G.; Bonn, M. Water Bending Mode at the Water−Vapor Interface Probed

by Sum-Frequency Generation Spectroscopy: A Combined Molecular Dynamics Simulation and Experimental Study. *J. Phys. Chem. Lett.* **2013**, *4*, 1872−1877.
(9) Ishiyama, T.; Morita, A. Molecular Dynamics Study of Gas-Liquid Aqueous Sodium Halide Interfaces. I. Flexible and Polarizable Molecular Modeling and Interfacial Properties. *J. Phys. Chem. C* **2007**, *111*, 721−737.
(10) Scatena, L. F.; Brown, M. G.; Richmond, G. L. Water at Hydrophobic Surfaces: Weak Hydrogen Bonding and Strong Orientation Effects. *Science* **2001**, *292*, 908−912.
(11) Smits, M.; Ghosh, A.; Sterrer, M.; Müller, M.; Bonn, M. Ultrafast Vibrational Energy Transfer between Surface and Bulk Water at the Air-Water Interface. *Phys. Rev. Lett.* **2007**, *98*, 098302.
(12) Eftekhari-Bafrooei, A.; Borguet, E. Effect of Hydrogen-Bond Strength on the Vibrational Relaxation of Interfacial Water. *J. Am. Chem. Soc.* **2010**, *132*, 3756−3761.
(13) Singh, P. C.; Nihonyanagi, S.; Yamaguchi, S.; Tahara, T. Communication: Ultrafast Vibrational Dynamics of Hydrogen Bond Network Terminated at the Air/Water Interface: A Two-Dimensional Heterodyne-Detected Vibrational Sum Frequency Generation Study. *J. Chem. Phys.* **2013**, *139*, 161101.
(14) Eftekhari-Bafrooei, A.; Borguet, E. Effect of Surface Charge on the Vibrational Dynamics of Interfacial Water. *J. Am. Chem. Soc.* **2009**, *131*, 12034−12035.
(15) Singh, P. C.; Nihonyanagi, S.; Yamaguchi, S.; Tahara, T. Ultrafast Vibrational Dynamics of Water at a Charged Interface Revealed by Two-Dimensional Heterodyne-Detected Vibrational Sum Frequency Generation. *J. Chem. Phys.* **2012**, *137*, 094706.
(16) Eftekhari-Bafrooei, A.; Borguet, E. Effect of Electric Fields on the Ultrafast Vibrational Relaxation of Water at a Charged Solid−Liquid Interface as Probed by Vibrational Sum Frequency Generation. *J. Phys. Chem. Lett.* **2011**, *2*, 1353−1358.
(17) Bonn, M.; Bakker, H. J.; Ghosh, A.; Yamamoto, S.; Sovago, M.; Campen, R. K. Structural Inhomogeneity of Interfacial Water at Lipid Monolayers Revealed by Surface-Specific Vibrational Pump-Probe Spectroscopy. *J. Am. Chem. Soc.* **2010**, *132*, 14971−14978.
(18) Zhang, Z.; Piatkowski, L.; Bakker, H. J.; Bonn, M. Ultrafast Vibrational Energy Transfer at the Water/Air Interface Revealed by Two-Dimensional Surface Vibrational Spectroscopy. *Nat. Chem.* **2011**, *3*, 888−893.
(19) Piatkowski, L.; Zhang, Z.; Backus, E. H. G.; Bakker, H. J.; Bonn, M. Extreme Surface Propensity of Halide Ions in Water. *Nat. Commun.* **2014**, *5*, 4083.
(20) Lock, A.; Bakker, H. Temperature Dependence of Vibrational Relaxation in Liquid H_2O. *J. Chem. Phys.* **2002**, *117*, 1708.
(21) Lock, A.; Woutersen, S.; Bakker, H. Ultrafast Energy Equilibration in Hydrogen-Bonded Liquids. *J. Phys. Chem. A* **2001**, *105*, 1238−1243.
(22) Liu, D.; Ma, G.; Levering, L. M.; Allen, H. C. Vibrational Spectroscopy of Aqueous Sodium Halide Solutions and Air- Liquid Interfaces: Observation of Increased Interfacial Depth. *J. Phys. Chem. B* **2004**, *108*, 2252−2260.
(23) Dlott, D. D. New Developments in the Physical Chemistry of Shock Compression. *Annu. Rev. Phys. Chem.* **2011**, *62*, 575−597.
(24) Dlott, D. D. Ultrafast Spectroscopy of Shock Waves in Molecular Materials. *Annu. Rev. Phys. Chem.* **1999**, *50*, 251−278.
(25) Querry, M. R.; Wieliczka, D. M.; Segelstein, D. J. Water (H_2O). In *Handbook of Optical Constants of Solids II*; Palik, E. D., Ed.; Elsevier Inc.: Amsterdam, 1991; pp 1059−1077.
(26) Backus, E. H. G.; Bonn, D.; Cantin, S.; Roke, S.; Bonn, M. Laser-Heating-Induced Displacement of Surfactants on the Water Surface. *J. Phys. Chem. B* **2012**, *116*, 2703−2712.
(27) Yang, F. *Study of Gigahertz Ultrasound Propagation in Water Using Picosecond Ultrasonics*; Brown University: Providence, RI, 2010.
(28) Lambert, A.; Davies, P.; Neivandt, D. Implementing the Theory of Sum Frequency Generation Vibrational Spectroscopy: A Tutorial Review. *Appl. Spectrosc. Rev.* **2005**, *40*, 103−145.
(29) Jungwirth, P.; Tobias, D. J. Ions at the Air/Water Interface. *J. Phys. Chem. B* **2002**, *106*, 6361−6373.
(30) Ishiyama, T.; Imamura, T.; Morita, A. Theoretical Studies of Structures and Vibrational Sum Frequency Generation Spectra at Aqueous Interfaces. *Chem. Rev.* **2014**, DOI: 10.1021/cr4004133.
(31) Tian, C.; Byrnes, S.; Han, H.-L.; Shen, Y. Surface Propensities of Atmospherically Relevant Ions in Salt Solutions Revealed by Phase-Sensitive Sum Frequency Vibrational Spectroscopy. *J. Phys. Chem. Lett.* **2011**, *2*, 1946−1949.